

Available online at www.sciencedirect.com

ScienceDirect

journal homepage: www.jfda-online.com

Original Article

Resveratrol protects muscle cells against palmitate-induced cellular senescence and insulin resistance through ameliorating autophagic flux

Yun-Ching Chang^a, Hung-Wen Liu^b, Yi-Tien Chen^{a,c}, Yun-An Chen^a, Yen-Ju Chen^a, Sue-Joan Chang^{a,*}

^a Department of Life Sciences, National Cheng Kung University, Tainan, Taiwan

^b Department of Physical Education, National Taiwan Normal University, Taipei, Taiwan

^c School of Food Safety, Taipei Medical University, Taipei, Taiwan

ARTICLE INFO

Article history:

Received 3 October 2017

Received in revised form

2 January 2018

Accepted 8 January 2018

Available online 3 February 2018

Keywords:

Autophagic flux

Resveratrol

Cellular senescence

Insulin resistance

ABSTRACT

Skeletal muscle, a highly metabolic tissue, is particularly vulnerable to increased levels of saturated free fatty acids (FFAs). The role of autophagy in saturated FFAs-induced cellular senescence and insulin resistance in skeletal muscle remains unclear. Therefore, the present study was aimed to explore autophagic flux in cellular senescence and insulin resistance induced by palmitate in muscle cells, and whether resveratrol limited these responses. Our results showed that palmitate induced cellular senescence in both myoblasts and myotubes. In addition, palmitate delayed differentiation in myoblasts and inhibited expression of insulin-stimulated p-AKTSer473 in myotubes. The accumulations of autophagosome assessed by tandem fluorescent-tagged LC3 demonstrated that autophagic flux was impaired in both palmitate-treated myoblasts and myotubes. Resveratrol protected muscle cells from palmitate-induced cellular senescence, apoptosis during differentiation, and insulin resistance via ameliorating autophagic flux. The direct influence of autophagic flux on development of cellular senescence and insulin resistance was confirmed by blockage of autophagic flux with chloroquine. In conclusion, impairment of autophagic flux is crucial for palmitate-induced cellular senescence and insulin resistance in muscle cells. Restoring autophagic flux by resveratrol could be a promising approach to prevent cellular senescence and ameliorate insulin resistance in muscle.

Copyright © 2018, Food and Drug Administration, Taiwan. Published by Elsevier Taiwan LLC. This is an open access article under the CC BY-NC-ND license (<http://creativecommons.org/licenses/by-nc-nd/4.0/>).

* Corresponding author. Department of Life Sciences, National Cheng Kung University, No. 1, University Road, Tainan, Taiwan. Fax: +886 6 2742583.

E-mail address: sjchang@mail.ncku.edu.tw (S.-J. Chang).

<https://doi.org/10.1016/j.jfda.2018.01.006>

1021-9498/Copyright © 2018, Food and Drug Administration, Taiwan. Published by Elsevier Taiwan LLC. This is an open access article under the CC BY-NC-ND license (<http://creativecommons.org/licenses/by-nc-nd/4.0/>).

1. Introduction

Skeletal muscle comprises 40–60% of total body mass and is responsible for almost 80% of whole body insulin-stimulated glucose disposal [1]. The long-term exposure of cells to high levels of free fatty acids (FFAs), particularly saturated FFAs such as palmitate, results in cellular senescence via promoting inflammation [2] and leads to deficiency of insulin-stimulated glucose uptake via PI3K-Akt signaling pathway [3]. Acceleration of cellular senescence and impairment of insulin pathway by palmitate eventually lead to a series of diseases such as obesity, type 2 diabetes, metabolic syndrome and cancer. However, the mechanisms underlying palmitate-induced cellular senescence and insulin resistance in muscle remain unclear.

Autophagy is a conserved cellular housekeeping process for the clearance of dysfunctional organelles and denatured proteins in living cells [4]. The autophagy-lysosome system is a degradation pathway that contributes to muscle protein degradation especially during muscle wasting [5]. Conversely, growing evidences indicate that autophagy is required to maintain muscle mass and regenerative function of muscle stem-cells [6,7]. These studies display a dual role of autophagy in muscle homeostasis. Several signaling pathways involved in cellular senescence and insulin resistance, including the mammalian target of rapamycin (mTOR) and AMP-activated protein kinase (AMPK), are reported to regulate autophagy [8,9]. The mTOR-dependent autophagy activators exhibit a potent anti-senescent effect through the restoration of autophagy [8]. Inactivation of the AKT/mTOR signaling impairs insulin signaling pathway and induces abnormal autophagosome formation [10,11]. These evidences indicate that impairment of autophagy may contribute to cellular senescence and insulin resistance.

Resveratrol, a natural polyphenol found in grapes and berries, exhibits a variety of biochemical and physiological effects including reversion of senescence process and amelioration insulin resistance [12]. It has been shown that resveratrol protects cellular senescence by reducing the production of ROS through the SIRT1/NADPH pathway [13] and improves glucose uptake and insulin sensitivity through SIRT1/AMPK pathway [14]. Recently, many studies have indicated that resveratrol is an autophagy regulator that exerts cardiovascular protection, neuroprotection, anti-inflammatory and anti-cancer effect by regulating autophagy [12,15–18]. Nonetheless, evidence linking resveratrol to underlying mechanisms of skeletal muscle regulated by autophagy is still lacking.

The objective of this study was to investigate the role of autophagy in palmitate-induced cellular senescence and insulin resistance in skeletal muscle. The efficacy of resveratrol in ameliorating cellular senescence and insulin resistance induced by palmitate via modulation of autophagy in C2C12 myoblasts and myotubes was further studied.

2. Methods

2.1. Materials

Resveratrol (RSV), palmitate (PA), chloroquine (CLQ) and other chemicals were from Sigma–Aldrich Chemical Co (St. Louis, MO, USA). For Western blotting, primary antibodies: p16, p21, p62 (Santa Cruz, CA, USA), LC3, AKT, phospho-AKT (Ser473), mTOR, phospho-mTOR (Ser2448), AMPK α , phospho-AMPK α (Thr172) (Cell signaling, Danvers, MA, USA), α -actin, GAPDH (GeneTex Inc., Hsinchu City, Taiwan), and caspase-9 (Millipore, Billerica, MA, USA) were commercially available. Goat anti-rabbit and sheep anti-mouse horseradish peroxidase (HRP) conjugated secondary antibodies were purchased from Bio-Rad (Hercules, CA, USA) and GE Healthcare Life Sciences (Pittsburgh, PA, USA).

2.2. Cell culture and treatment

C2C12 myoblasts were passaged in Dulbecco's modified Eagle's medium (DMEM) (Invitrogen, Carlsbad, CA, USA) supplemented with 10% fetal bovine serum (HyClone, Logan, UT, USA) under an atmosphere of 10% CO₂ in air at 37 °C. Twenty-four hours after seeding, myoblasts were pretreated with or without 100 μ M resveratrol for 16 h, and then incubated with 250 μ M palmitate for 24 h (Fig. 3A).

When the myoblasts reached approximately 80% confluency, they were differentiated into myotubes in DMEM containing 2% horse serum (Invitrogen, Carlsbad, CA, USA), with medium changes every two days. After five days differentiation, differentiated myotubes were pretreated with or without 100 μ M resveratrol for 16 h, and then incubated with 250 μ M palmitate for 24 h (Fig. 4A).

There was no evidence for toxicity of resveratrol to myoblasts and myotubes at the concentrations employed in this study based on cell viability assay by MTT (data not show).

2.3. β -galactosidase staining

β -galactosidase activity was determined using the Senescence Detection Kit (BioVision, Milpitas, CA, USA) according to a standard protocol. Images were observed under the phase contrast microscopy and captured with a digital camera (Nikon Corporation, Tokyo, Japan). Four random fields were counted to determine the percentage of β -galactosidase-positive cells in the total cell population.

2.4. MTT assay

MTT (3-[4, 5-dimethylthiazol-2, 5-diphenyl tetrazolium bromide) assay was carried out for assessment of the growth curves. MTT dissolved in PBS at 5 mg/ml was added to the culture medium at a dilution 1:10. The cell in the number of 5000, 10,000, 20,000, 40,000, 80,000 and 16,0000 were incubated for depicting standard curve, and 10,000 cells were incubated for assessing. After 4 h incubation period with MTT, medium

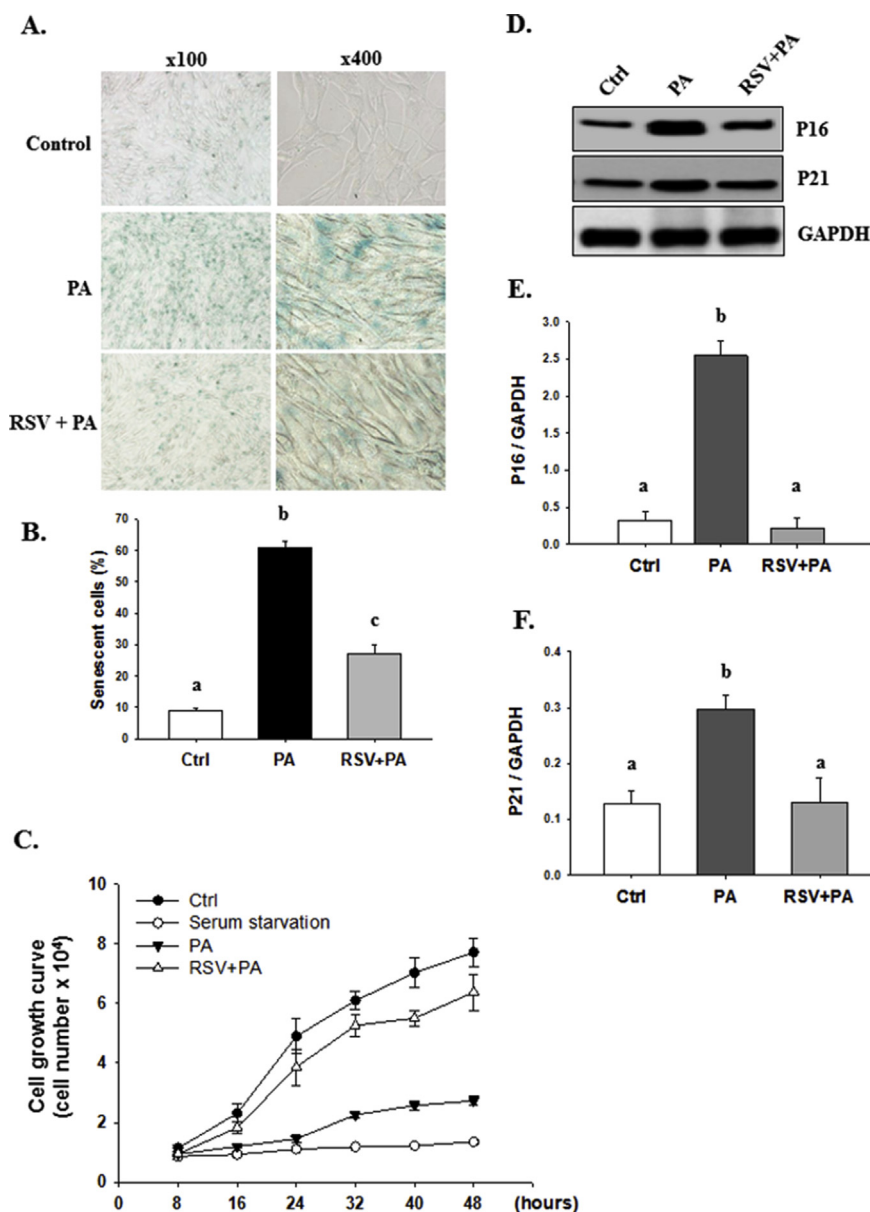


Fig. 1 – (A) Representative images of β -galactosidase staining (magnification $\times 100$ and $\times 400$). (B) Quantification of β -galactosidase positive cells stained with blue color. The values are the means \pm SEM for 500 myoblasts in each group. (C) Cell growth curves of C2C12 myoblasts. (D) Representative blots of P16 and P21. Quantification of (E) P16 and (F) P21 normalized with GAPDH ($n = 4$ /group). Significance ($p < 0.05$) among groups is denoted by different letters.

was aspirated and DMSO was added to extract the MTT formazan. The absorbance of each well was detected by micro plate reader (TECAN, Richmond, USA) at the wavelength of 540 nm.

2.5. Western blotting

Total protein in the supernatant was measured by the BCA method (Bio-Rad). An equal amount of protein for each preparation was separated by SDS-PAGE, transferred to PVDF membrane, blocked with 5% nonfat dry milk in 0.1% Tween-Tris buffered saline (TBST), and incubated with different primary antibodies in TBST. Membranes were then washed

and incubated with HRP-conjugated secondary antibodies in TBST. Protein bands were visualized using a Chemiluminescence kit (Millipore). Quantitative results of Western blotting were performed using the LAS-4000 mini biomolecular imager (GE Healthcare Life Sciences).

2.6. Detection of autophagic flux

To evaluate autophagic flux, C2C12 cells were detected using the Premo™ Autophagy Tandem Sensor RFP-GFP-LC3B Kit (Thermo Fischer Scientific, Grand Island, NY, USA) as described in the manufacturer's protocol. By combining an acid-sensitive GFP with an acid insensitive RFP, the change

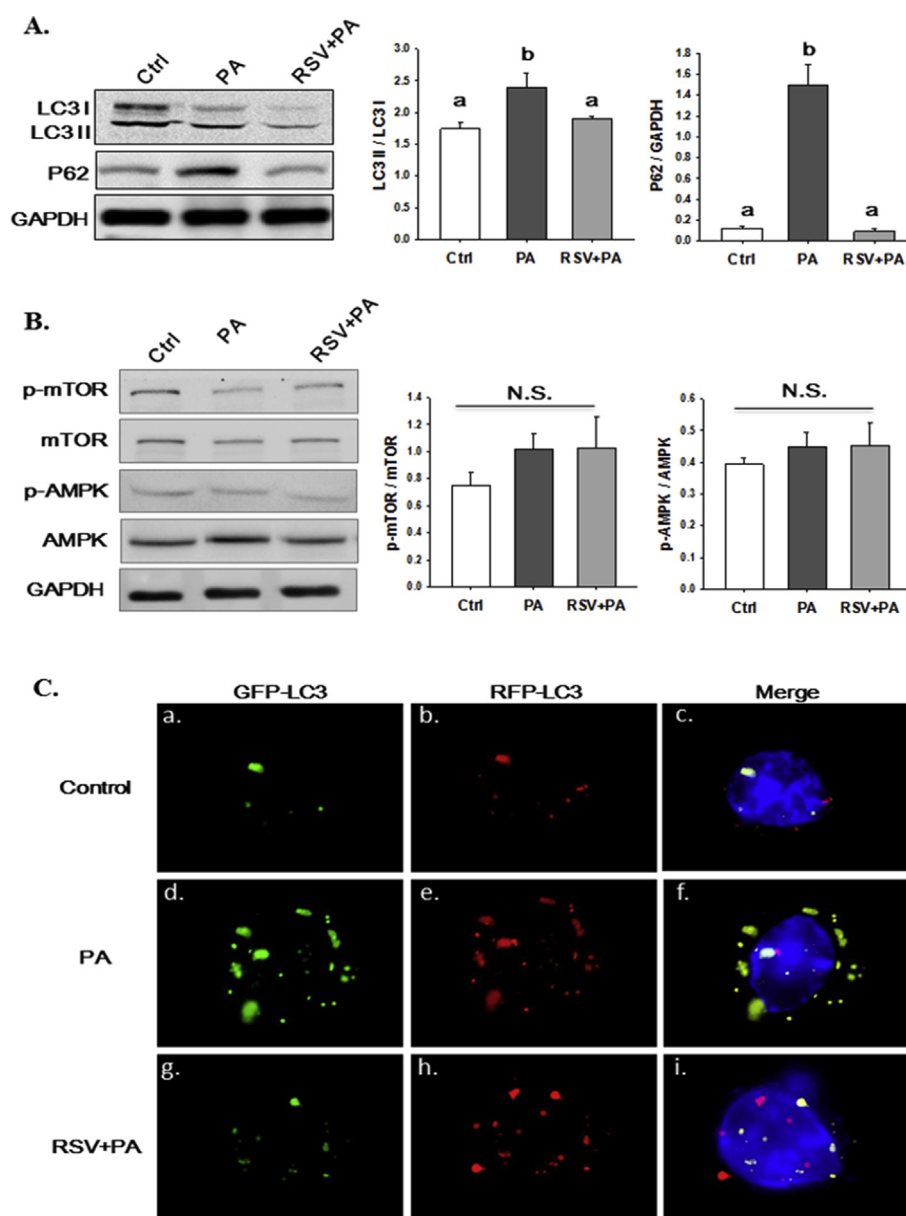


Fig. 2 – Representative blots and quantification of (A) LC3-I, LC3-II, P62. (B) mTOR, p-mTOR^{Ser2447}, AMPK and p-AMPK^{Thr172} (n = 4/group) (C) Fluorescence images of mRFP-GFP-LC3 (magnification $\times 400$). The transition from the autophagosome (yellow) to the autolysosome (red) can be visualized by the specific loss of GFP fluorescence. Significance ($p < 0.05$) among groups is denoted by different letters. N.S. = no significance.

from autophagosome (neutral pH) to autolysosome (with an acidic pH) can be visualized by imaging the specific loss of the GFP fluorescence, leaving only red fluorescence. In brief, the cells were grown to 60% confluency on cover slips prior to transfection. Then, the cells were incubated with BacMam Reagents containing the RFP-GFP-LC3B overnight. Fluorescent images were taken using microscopy and captured with a digital camera (Nikon Corporation).

2.7. Crystal violet staining

Cells were fixed with 4% paraformaldehyde for 10 min, then stained with 0.5% crystal violet for 5 min, and washed

three times with water. The images were taken using microscopy and captured with a digital camera (Nikon Corporation).

2.8. Statistical analysis

Data were expressed as means \pm SEM from at least three independent experiments for each group. The statistical significance of different groups was determined by one-way ANOVA or Student's t-test with Sigma Plot 12.0 (San Jose, CA, USA). The post Hoc test was used if the ANOVA was significant. $P < 0.05$ was considered statistically significant.

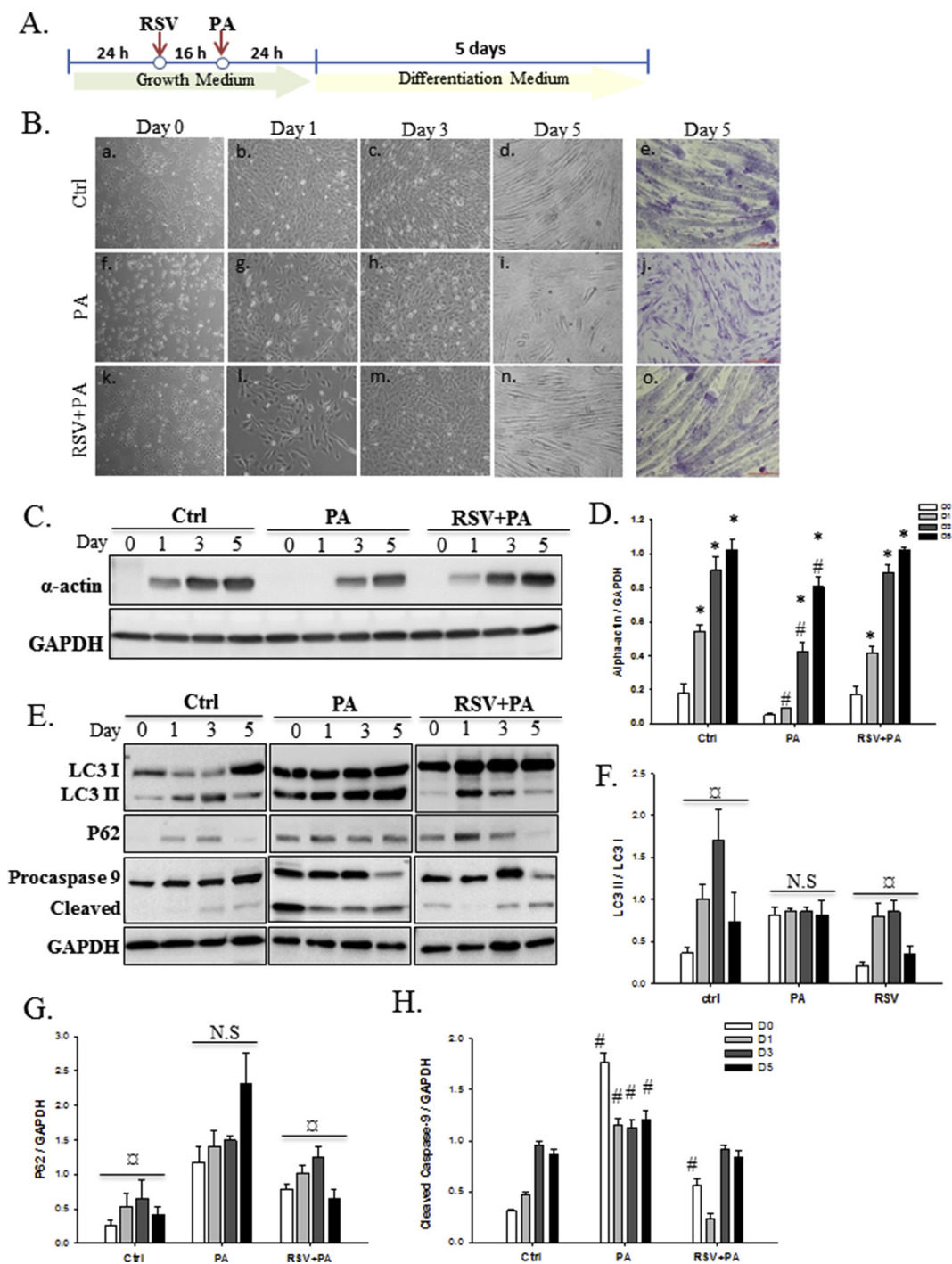


Fig. 3 – (A) Schematic diagram of experimental design. (B) Representative images of myotube differentiation up to 5 d (a–d, f–i, and k–n, phase contrast, magnification $\times 100$) (e, j, and o, crystal violet staining, magnification $\times 400$). (C) Representative blots and (D) quantification of α -actin ($n = 3/\text{group}$). (E) Representative blots and (F–H) quantification of LC3-I, LC3-II, P62 and caspase 9 ($n = 3/\text{group}$) (D, F–H) * $p < 0.05$ compared with d0. # $p < 0.05$ compared with ctrl. *Significantly different ($p < 0.05$) among groups. N.S. = no significance.

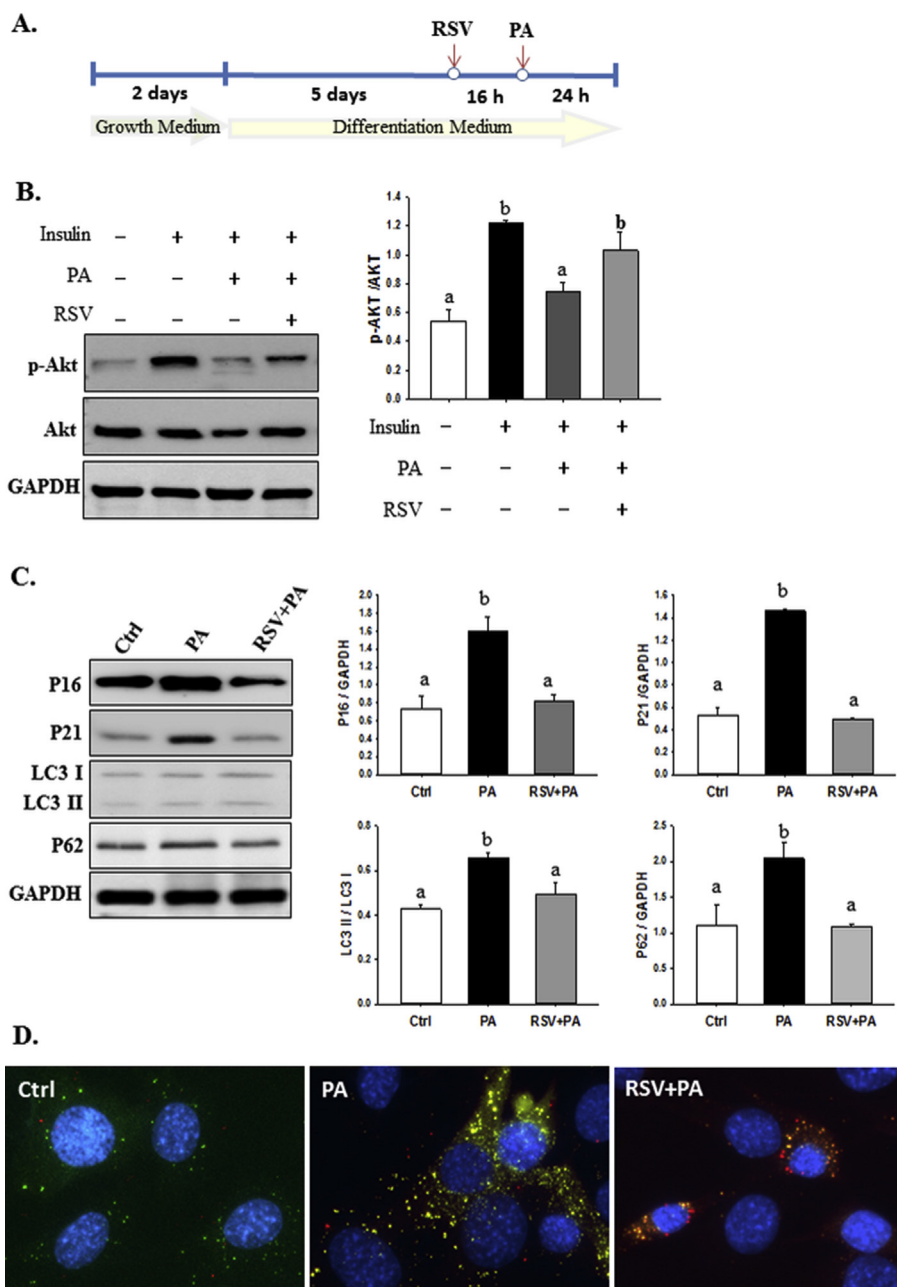


Fig. 4 – (A) Schematic diagram of experimental design. (B) Representative blots and quantification of Akt and p-Akt^{Ser473} (n = 4/group). (C) Representative blots and quantification of P16, P21, LC3-I, LC3-II, and P62 (n = 4/group). (D) Fluorescence images of mRFP-GFP-LC3 (magnification ×200). The transition from the autophagosome (yellow) to the autolysosome (red) can be visualized by the specific loss of GFP fluorescence. Significance (p < 0.05) among groups is denoted by different letters.

3. Results

3.1. Resveratrol protects C2C12 myoblasts from palmitate-induced cellular senescence

The expression of senescence-associated beta-galactosidase was significantly increased in palmitate-treated cells and considerably decreased by resveratrol pre-treatment (Fig. 1A and B). Cell growth arrest (Fig. 1C) and increased expressions

of P16 and P21 (Fig. 1D–F), the key proteins involved in cell cycle, were observed in palmitate-treated and significantly limited in resveratrol-pretreated cells.

3.2. Resveratrol ameliorates autophagic flux in palmitate-treated C2C12 myoblasts

The expression of autophagy markers, LC3-I and LC3-II, and autophagy regulating protein, P62, were significantly

increased in palmitate-treated cells and reversed by resveratrol pre-treatment (Fig. 2A). However, there were no significant differences in activities of AMPK and mTOR among three groups (Fig. 2B). Furthermore, C2C12 myoblasts were transfected with pH-sensitive mRFP-GFP-LC3-plasmid to monitor autophagic flux. A significant increase in the ratio of yellow:red puncta was observed in palmitate-treated cells (Fig. 2C.f), reflecting a blockage in the fusion of autophagosomes with lysosomes. The yellow:red puncta was significantly declined in resveratrol-pretreated cells (Fig. 2C.i), indicating resveratrol ameliorated autophagic flux in palmitate-induced senescent C2C12 myoblasts.

3.3. Resveratrol protects against palmitate-induced apoptosis during differentiation

The effect of palmitate on C2C12 differentiation and the efficacy of resveratrol to limit this response were further investigated. C2C12 myoblasts were incubated with or without resveratrol for 16 h and treated with palmitate for 24 h. After treatment, C2C12 myoblasts were switched from growth medium to differentiation medium to induce differentiation (Fig. 3A). Palmitate inhibited myotubes formation (Fig. 3B a–e vs. f–j) and delayed skeletal muscle α -actin expression (Fig. 3C and D) compared with control cells. Resveratrol significantly restored myotubes formation (Fig. 3B f–j vs. k–o) and skeletal muscle α -actin expression (Fig. 3C and D) during differentiation. Furthermore, expression of LC3-II and P62 display a dynamic change which increased from 1st to 3rd day and degraded at the 5th day (Fig. 3E–G) in control and resveratrol-pretreated cells. However, accumulations of LC3-II and P62 accompanied with a high level of cleaved caspase-9 was observed in palmitate-treated cells (Fig. 3E–G).

3.4. Resveratrol prevents C2C12 myotubes from palmitate-induced cellular senescence and insulin resistance

C2C12 myotubes were used to determine the efficacy of resveratrol on palmitate-induced cellular senescence and insulin resistance. After five days differentiation, differentiated myotubes were pretreated with or without resveratrol for 16 h, and then incubated with palmitate for 24 h (Fig. 4A). The insulin-stimulated p-AKT^{Ser473} was inhibited in palmitate-treated myotubes (Fig. 4B, Lane 3) and markedly prevented by resveratrol pre-treatment (Fig. 4B, Lane 4). Consistently, expressions of P16, P21, LC3-II and P62 were increased in palmitate-treated myotubes and significantly decreased by resveratrol pre-treatment (Fig. 4C). The ratio of yellow:red puncta was elevated in palmitate-treated myotubes and declined in resveratrol-pretreated myotubes (Fig. 4D). Taken together, resveratrol prevents cellular senescence, insulin resistance and autophagic flux in palmitate-treated C2C12 myotubes.

3.5. Blockage of autophagic flux induces cellular senescence and insulin resistance

To confirm whether direct impairment of autophagic flux induces cellular senescence and insulin resistance, a lysosome

inhibitor capable of blocking autophagic protein degradation, chloroquine (CLQ), was used. The β -galactosidase-positive cells were increased in both C2C12 myoblasts and myotubes when treated with CLQ (Fig. 5A). The length of myotube was significantly decreased in CLQ-treated myotubes compared with control myotubes (Fig. 5B). Moreover, a decrease in the level of insulin-stimulated p-AKT^{Ser473} was observed in CLQ-treated myotubes (Fig. 5C). These results indicate that impairment of autophagic flux directly induces cellular senescence and insulin resistance in muscle cells.

4. Discussion

The significant findings of the present study include that (1) blockage of autophagic flux directly induces cellular senescence and insulin resistance, (2) palmitate impairs autophagic flux resulting in cellular senescence and insulin resistance in muscle cells, and (3) resveratrol as a promising agent protects muscle cells against cellular senescence and insulin resistance via restoration of autophagic flux.

Insulin resistance is recognized as an important risk factor in the development of type II diabetes, and is generally related to the Western-type diet high in saturated FFAs [19–21]. Increasing evidences reveal that excessive fat exposure influences autophagy and results in cellular senescence and insulin resistance [22,23]. However, autophagy may play a dual role during these processes. Marked conversion of LC3-I to LC3-II was observed in the insulin resistant β cells induced by high fat diet (HFD) and FFAs, suggesting that autophagy is positively correlated with insulin resistance [24]. Conversely, Singh et al. reported that hepatic autophagy was suppressed in insulin resistance shown by decreased LC3-II and increased p62 protein expressions [25].

Autophagy is a dynamic process that comprises sequential stages including formation of phagophore, formation of autophagosomes, fusion of autophagosomes with lysosomes and degradation [8]. The status of autophagy is affected by many factors such as cell type, inducer, and measuring time point. Therefore, the real status of autophagy should be monitored not only by quantitative expression of autophagy markers but also by status of the autophagic flux [8,26,27]. In the present study, we found that palmitate induced expression of LC3-II and P62 in both myoblasts and myotubes (Figs. 2A and 4C). Simultaneously, autophagosome accumulations clarified by the elevated yellow puncta of mRFP-GFP-LC3 fluorescence were observed in palmitate-treated myoblasts and myotubes (Figs. 2C and 4D). However, AMPK and mTOR, the regulators of phagophore formation, were not significantly changed (Fig. 2B). These data suggested that palmitate impaired autophagy resulted from deficient fusion between autophagosomes and lysosomes, but not the initiation of autophagy. He et al. described similar patterns of dysregulation in skeletal muscle of wild-type C57BL/6 mice following a HFD for 12 weeks. Their data showed that lipidation of LC3 was inhibited in HFD mice, indicating an error in autophagosome maturation or lysosome fusion [28]. Together, excessive fat exposure results in abnormal autophagic flux in skeletal muscle, leading to cellular senescence and insulin resistance.

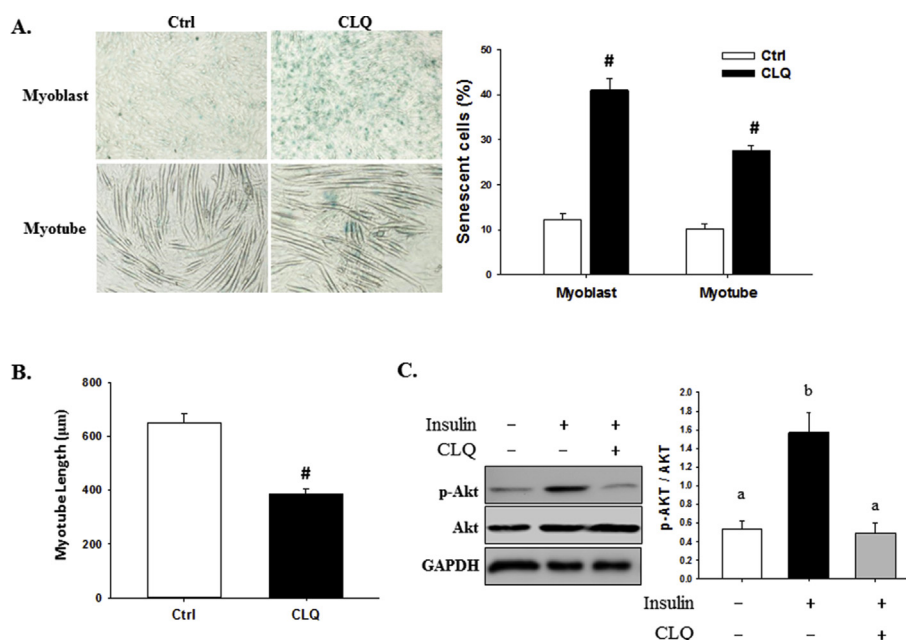


Fig. 5 – (A) Representative images and quantification of β -galactosidase staining (magnification $\times 100$) ($n = 4/\text{group}$). (B) Quantification of average myotube length. The single myotube length was measured using ImageJ software. (C) Representative blots and quantification of Akt and p-Akt^{Ser473} ($n = 4/\text{group}$). # $P < 0.05$ compared with ctrl. Significance ($p < 0.05$) among groups is denoted by different letters.

The therapeutic implication of ameliorating autophagic flux in diseases has been noticed [8,11,29]. Accumulation of autophagosomes altered amyloid precursor protein processing, leading to increased amyloid β peptide generation, which might be involved in the pathogenesis of Alzheimer's disease [11]. Our results confirmed the direct effect of autophagic flux on cellular senescence and insulin resistance in myoblasts and myotubes (Fig. 5), indicating that autophagic flux is a potential therapeutic target for cellular senescence and insulin resistance in skeletal muscle. Recently, resveratrol is reported to regulate autophagy through different mechanisms such as activation of AMPK and SIRT1, up-regulation of Atg5 and Atg12 genes expression, and increasing LC3 lipidation [30–32]. In the present study, we demonstrated that resveratrol reduced autophagosome accumulations in palmitate-treated myoblasts and myotubes. Restoring autophagic flux by resveratrol significantly mitigated cellular senescence and ameliorated insulin resistance induced by palmitate. Previous research has shown that autophagy protects differentiating myoblasts from apoptotic cell death [33]. We also found that palmitate blocked autophagic flux during myoblasts differentiation and resulted in apoptosis. Resveratrol protects differentiating myoblasts from apoptotic cell death via ameliorating autophagic flux (Fig. 3E–H).

In conclusion, our results suggest autophagosome accumulations induced by palmitate impair autophagic flux leading to cellular senescence and insulin resistance in muscle cells. Resveratrol acts as an autophagy modulator to protect muscle cell against palmitate-induced cellular senescence and insulin resistance.

Funding

This research was supported by a grant from the Ministry of Science and Technology, Taiwan, to S.-J.C (104-2320-B-006-023-MY3).

Conflicts of interest

The authors declare that they have no conflicts of interest.

REFERENCES

- [1] Yang M, Wei D, Mo C, Zhang J, Wang X, Han X, et al. Saturated fatty acid palmitate-induced insulin resistance is accompanied with myotube loss and the impaired expression of health benefit myokine genes in C2C12 myotubes. *Lipids Health Dis* 2013;12:104.
- [2] Sokolova M, Vinge LE, Alfsnes K, Olsen MB, Eide L, Kaasboll OJ, et al. Palmitate promotes inflammatory responses and cellular senescence in cardiac fibroblasts. *Biochim Biophys Acta* 2017;1862:234–45.
- [3] Dey D, Basu D, Roy SS, Bandyopadhyay A, Bhattacharya S. Involvement of novel PKC isoforms in FFA induced defects in insulin signaling. *Mol Cell Endocrinol* 2006;246:60–4.
- [4] Kim KH, Lee MS. Autophagy—a key player in cellular and body metabolism. *Nat Rev Endocrinol* 2014;10:322–37.
- [5] Sandri M. Protein breakdown in muscle wasting: role of autophagy-lysosome and ubiquitin-proteasome. *Int J Biochem Cell Biol* 2013;45:2121–9.

- [6] Sandri M. Autophagy in skeletal muscle. *FEBS Lett* 2010;584:1411–6.
- [7] Fiacco E, Castagnetti F, Bianconi V, Madaro L, De Bardi M, Nazio F, et al. Autophagy regulates satellite cell ability to regenerate normal and dystrophic muscles. *Cell Death Differ* 2016;23:1839–49.
- [8] Tai H, Wang Z, Gong H, Han X, Zhou J, Wang X, et al. Autophagy impairment with lysosomal and mitochondrial dysfunction is an important characteristic of oxidative stress-induced senescence. *Autophagy* 2017;13:99–113.
- [9] Han X, Tai H, Wang X, Wang Z, Zhou J, Wei X, et al. AMPK activation protects cells from oxidative stress-induced senescence via autophagic flux restoration and intracellular NAD(+) elevation. *Aging Cell* 2016;15:416–27.
- [10] Young JE, Martinez RA, La Spada AR. Nutrient deprivation induces neuronal autophagy and implicates reduced insulin signaling in neuroprotective autophagy activation. *J Biol Chem* 2009;284:2363–73.
- [11] Son SM, Song H, Byun J, Park KS, Jang HC, Park YJ, et al. Altered APP processing in insulin-resistant conditions is mediated by autophagosome accumulation via the inhibition of mammalian target of rapamycin pathway. *Diabetes* 2012;61:3126–38.
- [12] Tsai HY, Ho CT, Chen YK. Biological actions and molecular effects of resveratrol, pterostilbene, and 3'-hydroxypterostilbene. *J Food Drug Anal* 2017;25:134–47.
- [13] Tang Y, Xu J, Qu W, Peng X, Xin P, Yang X, et al. Resveratrol reduces vascular cell senescence through attenuation of oxidative stress by SIRT1/NADPH oxidase-dependent mechanisms. *J Nutr Biochem* 2012;23:1410–6.
- [14] Breen DM, Sanli T, Giacca A, Tsiani E. Stimulation of muscle cell glucose uptake by resveratrol through sirtuins and AMPK. *Biochem Biophys Res Commun* 2008;374:117–22.
- [15] Fu DG. Regulation of redox signalling and autophagy during cardiovascular diseases-role of resveratrol. *Eur Rev Med Pharmacol Sci* 2015;19:1530–6.
- [16] Wu Y, Li X, Zhu JX, Xie W, Le W, Fan Z, et al. Resveratrol-activated AMPK/SIRT1/autophagy in cellular models of Parkinson's disease. *Neurosignals* 2011;19:163–74.
- [17] Andreadi C, Britton RG, Patel KR, Brown K. Resveratrol-sulfates provide an intracellular reservoir for generation of parent resveratrol, which induces autophagy in cancer cells. *Autophagy* 2014;10:524–5.
- [18] Wu J, Li X, Zhu G, Zhang Y, He M, Zhang J. The role of Resveratrol-induced mitophagy/autophagy in peritoneal mesothelial cells inflammatory injury via NLRP3 inflammasome activation triggered by mitochondrial ROS. *Exp Cell Res* 2016;341:42–53.
- [19] Del Toro-Equihua M, Velasco-Rodriguez R, Lopez-Ascencio R, Vasquez C. Effect of an avocado oil-enhanced diet (*Persea americana*) on sucrose-induced insulin resistance in Wistar rats. *J Food Drug Anal* 2016;24:350–7.
- [20] Zimmet P, Alberti KG, Shaw J. Global and societal implications of the diabetes epidemic. *Nature* 2001;414:782–7.
- [21] Hommelberg PP, Plat J, Sparks LM, Schols AM, van Essen AL, Kelders MC, et al. Palmitate-induced skeletal muscle insulin resistance does not require NF-kappaB activation. *Cell Mol Life Sci* 2011;68:1215–25.
- [22] Park HW, Park H, Semple IA, Jang I, Ro SH, Kim M, et al. Pharmacological correction of obesity-induced autophagy arrest using calcium channel blockers. *Nat Commun* 2014;5.
- [23] Koga H, Kaushik S, Cuervo AM. Altered lipid content inhibits autophagic vesicular fusion. *Faseb J* 2010;24:3052–65.
- [24] Ebato C, Uchida T, Arakawa M, Komatsu M, Ueno T, Komiya K, et al. Autophagy is important in islet homeostasis and compensatory increase of beta cell mass in response to high-fat diet. *Cell Metabol* 2008;8:325–32.
- [25] Singh R, Kaushik S, Wang YJ, Xiang YQ, Novak I, Komatsu M, et al. Autophagy regulates lipid metabolism. *Nature* 2009;458:1131–U64.
- [26] Loos B, du Toit A, Hofmeyr JH. Defining and measuring autophagosome flux-concept and reality. *Autophagy* 2014;10:2087–96.
- [27] Mizushima N, Yoshimori T, Levine B. Methods in mammalian autophagy research. *Cell* 2010;140:313–26.
- [28] He CC, Bassik MC, Moresi V, Sun K, Wei YJ, Zou ZJ, et al. Exercise-induced BCL2-regulated autophagy is required for muscle glucose homeostasis. *Nature* 2012;481:511–U126.
- [29] Liu PF, Leung CM, Chang YH, Cheng JS, Chen JJ, Weng CJ, et al. ATG4B promotes colorectal cancer growth independent of autophagic flux. *Autophagy* 2014;10:1454–65.
- [30] Mauthe M, Jacob A, Freiburger S, Hentschel K, Stierhof YD, Codogno P, et al. Resveratrol-mediated autophagy requires WIPI-1 regulated LC3 lipidation in the absence of induced phagophore formation. *Autophagy* 2011;7:1448–61.
- [31] Chang CH, Lee CY, Lu CC, Tsai FJ, Hsu YM, Tsao JW, et al. Resveratrol-induced autophagy and apoptosis in cisplatin-resistant human oral cancer CAR cells: a key role of AMPK and Akt/mTOR signaling. *Int J Oncol* 2017;50:873–82.
- [32] Ma LQ, Fu RG, Duan ZY, Lu JM, Gao J, Tian LF, et al. Sirt1 is essential for resveratrol enhancement of hypoxia-induced autophagy in the type 2 diabetic nephropathy rat. *Pathol Res Pract* 2016;212:310–8.
- [33] McMillan EM, Quadrilatero J. Autophagy is required and protects against apoptosis during myoblast differentiation. *Biochem J* 2014;462:267–77.